Article

Inelastic Scattering Imaging System for *Pseudocercospora fijiensis* Detection

Juan Velez-Alvarez [1,†,‡] (iD)**, Alvaro Bastidas** [2,‡]**, Alejandra Monsalve** [3,]**, Tehseen Adel** [4]**, Isabel Calle-Balbin** [5,] **and Rafael Arango** [6,]

[1]   Universidad Nacional de Colombia sede Medellin; jevelezal@unal.edu.co
[2]   Universidad Nacional de Colombia sede Medellin; aebastid@unal.edu.co
[3]   Universidad Nacional de Colombia sede Medellin; amonsalver@unal.edu.co
[4]   The Ohio State University; adel.4@buckeyemail.osu.edu
[5]   Universidad Nacional de Colombia sede Medellin; iccalleb@unal.edu.co
[6]   Universidad Nacional de Colombia sede Medellin; rearango@unal.edu.co
*   Correspondence: jevelezal@unal.edu.co; Tel.: +57-4-3506175210
†   Current address: Affiliation 3
‡   These authors contributed equally to this work.

Version June 17, 2019 submitted to Journal Not Specified

1   **Abstract:** This work sought to develop an inelastic scattering imaging system based on Raman
2   spectroscopy for the detection of the fungal phytopathogen, *Pseudocercospora fijiensis*, which causes
3   Black Sigatoka disease in banana crops, very important in Colombian agro-industrial economy. This
4   system consists of a modified stereoscope with an optical setup able to simultaneously capture spectral
5   images together with its Raman spectra. The camera has two different bandpass filters attached, centered
6   in the spectral region of C=O stretching of Chitin and the equatorial bending vibration of $\beta-1,3$-glucan,
7   molecules of the fungal cell wall. In this way, the system can get images with unique spectral features,
8   suitable for training a convolutional neural network in order to get a recognition pattern of the fungal
9   strain growing in the PDA agar. As a result, the instrument was able to detect the presence of *P.fijiensis*
10 over the culture media.

11 **Keywords:** Inelastic Scattering; *P.fijiensis*; Banana; phytopathogen; deep learning

12 **1. Introduction**

13   The different varieties of banana, belonging to the genus Musa, are one of the most important crops in
14 the tropical and subtropical regions of the world [1]. This crop is attacked by several diseases among Black
15 Sigatoka (BS) is one of them, which is caused by the fungus Ascomycete *Pseudocercospora fijiensis* (Synonym:
16 *Mycosphaerella fijiensis*), this fungus attacks the leaves of plants of the genus Musa, causing foliar spots
17 that widen with the course of the disease [2], decreasing the photosynthetic capacity of the plant, which
18 translates into a lower growth and early maturation [3]. This disease was first described in 1964 on the
19 island of Fiji in Southeast Asia (Rhodes, 1964) spreading to all banana crops around the world reaching
20 America around 1972 [5]. In the case of Colombia, export bananas have become one of the most important
21 crops in the country. In 2014, according to data from FAOSTAT (FAO, 2017), Colombia had more than
22 73,000 hectares (hectares) of bananas planted and production of 1'770,899 tons a year of bananas, ranking
23 third in the Colombian economy after coffee and flowers and thus contributing to 0.4% of GDP [6]. One of
24 the greatest challenges is to reduce the use of fungicides since it increases the production costs by 13.8%

25 and reduces competitiveness in highly demanding markets regarding the presence of these substances
26 [8], for this reason a device able to supply an effective tool for the detection of *P.fijiensis* was designed by
27 getting the inelastic scattering signature of two molecules of the fungal cell wall, for the purposes of this
28 work chitin and $\beta - 1,3$-glucan were selected to provide evidence about the presence of this organisms,
29 [9], for instance the latter molecule is considered a molecular bio-marker for fungi [10]. Raman inelastic
30 scattering was selected for primarily two reasons, (i) there is no need for sample preparation, and (ii) a
31 spectral fingerprint region associated with the molecular structure of the sample can be obtained. The
32 phenomenon, known as polarizability, is associated with the interaction of the molecular cluster with an
33 electric field. Electrons move to opposite directions creating a temporal dipole and oscillation frequency
34 [12] [11], the oscillation frequency, and the amplitude defines a very specific organic functional group,
35 the linear combination of oscillations and amplitudes is exclusive of each molecule in the region between
36 [200-1800] cm^{-1} [13]. Using two filters, the first in the spectral region of (788.78-939.85) cm^{-1} associated
37 with the equatorial bending vibrations and covers both alpha and beta type carbohydrate monomers. In
38 particular, the 893 cm^{-1} band which is considered a marker for beta-glucans [15], [16]. The second filter
39 was selected for the detection of chitin, which has two Raman peaks in the region of (1600-1700) cm^{-1}
40 which corresponds to amid I group due to C=O stretching vibrations of the peptide bond [14]. By selecting
41 filters that match the bio-marked criteria it is possible to have an exclusive signal of the phytopathogen by
42 taking images composed of the intensities of the peaks at the corresponding spectral band. By selecting
43 chitin and beta-1,3-glucan, evidence for the presence of the phytopathogen can be ascertained. This
44 fingerprint makes possible to run image recognition algorithms, usually, this task is traditionally relied
45 on in PCA (Principal components analysis) [17], [18], but in this work, the technique selected was a deep
46 learning algorithm, called convolutional neural networks, which is mainly used in image processing. The
47 platform selected for that task was Tensorflow implemented over Python, that gives access to one of the
48 most powerful image classification systems: PNASNET-5 (Progressive Neural Architecture Search) one of
49 the latest and fastest architectures for pattern recognition, based on a sequential optimization by increasing
50 the level of complexity each time an image is added [19][20]. The combination of deep learning together
51 with the use of Raman scattering made it possible to achieve a detection with a confidence level above
52 90%.

2. Materials and Methods

2.1. Plant material

55 Black-leaf-streak-susceptible Williams (triploid, AAA genome group) plants were obtained from
56 the in vitro culture facilities of the Plant Biotechnology Unit Universidad Catolíca de Oriente, Rionegro,
57 Colombia. Two-month-old plants were kept under greenhouse conditions at 29°C and relative humidity
58 (RH) above 95% with standard fertilization and irrigation practices until inoculation.

2.2. Pseudocercospora fijiensis strains

60 Two isolates of P.fijiensis (C139 and 080930) from the collection of isolates of the Group-Biotecnología
61 Vegetal Unalmed -CIB were used for the infection. Those fungi were grown on potato dextrose agar (Difco,
62 Becton Dickinson, Franklin Lakes, NJ) and incubated at 25± 1°C until a colony of about 1 cm in diameter
63 was obtained.
64 Inoculation of banana with mycelial fragments of P.fijiensis was performed as reported in [36]. After
65 inoculation, plants were kept in an infection chamber at constant temperature of 29°C, RH of 95%, and 12
66 h of light and 12 h of darkness. Fragments of infected leaves of an approximate area of 1 square centimeter
67 were used to determine the presence of the fungus. an uninfected leaf was also used as control.

2.3. Optical Setup

The optical setup consists of two different microscopes, a Boeco^{TM} stereoscope and a Rossbach^{TM} microscope, the former was used as the optical stage, it brings a 10x optical magnification suitable to study peel and leaves injuries were is more likely to find an infection process by a fungal strain [37]. The Rossbach^{TM} microscope in the other hand was used to supply the positioning stage of the optical system, specifically, the laser and sample alignment, the x,y mechanism, and the coarse and fine focus knobs.

The microscope eyepieces were coupled with a spectrometer and a camera. The former is a B&W Tek ^{TM} (Model BTC-110S), with a spectral range of $(400\text{-}2500)cm^{-1}$ and a dynamic range of 30dB. The camera on the other hand is a FLIR^{TM} *Flea 3* Gigabit Ethernet, containing a CCD ICX 655 Sony^{TM} sensor with a quantum efficiency of 50% for the green channel, 54dB of dynamic range and a temporal dark noise of $7.45e^{-}$, those specifications are ideal to get very low optical intensity signals. This sensor came without focusing lenses, for that reason a 4x Rossbach objective was used for this task.

The filtering section is conformed by a Thorlabs^{TM} laser line filter with a FWHM of 3nm, two bandpass filters Omega.Inc centered at 578 nm and 557 nm with a FWHM of 8 nm and 5nm respectively. The dichroic mirror obtained from an Epson^{TM} projector whose spectral response at $45°$ can be seen in figure 1 was combined with a Omega.Inc Rapid Edge filter (cut-on=540nm) to reduce the Rayleigh backstering signal.
It is important to mention that the laser was modified in order to get a wider spot, by removing the collimating lenses. Originally the spot was 5mm in diameter but after the modification the size increase to 9mm due to the divergence angle of the laser diode ($5°$), this was made in order to encompass a broader area.
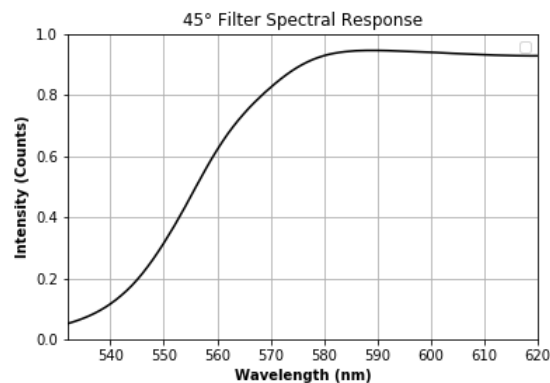

Figure 1. Spectral Response of the $45°$ long-pass filter

3. Results and Discussion

The following setup was designed to simultaneously obtain an image and a spectrum in order to associate the picture taken by the camera with the spectral information produced by the interaction of the laser light and sample.

3.1. Optical Setup

Figure 2 shows the components and the different optical elements of the device, it is comprised of a 532nm laser diode and a Thorlabs^{TM} laser line filter, CWL = 532 ± 0.6 nm, FWHM = 3 ± 0.6 nm attached to the optical output, this arrangement reduces the spectral bandwidth of the laser, after that, the laser beam is then deflected by a high pass filter at $45°$, with a cut-on wavelength of 550nm. Once the sample is illuminated, an excitation in the molecules is produced temporarily generating an induced dipole, this dipole can oscillate with the same frequency of the incident photon, producing Rayleigh scattering
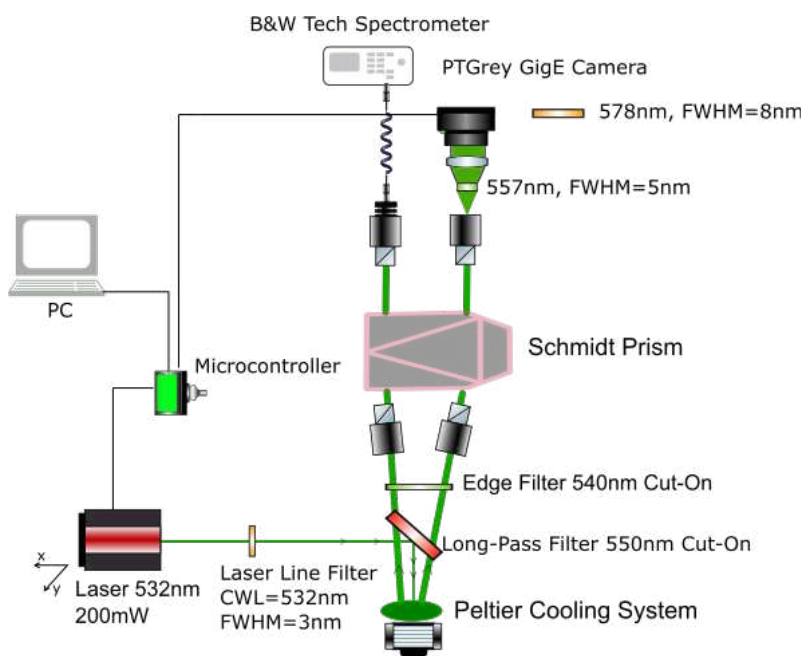

Figure 2. Micro Raman Setup

The emerging photons may have a slightly different energy value, which is dependent on the type of molecules present in the sample (polarizability), this type of scattering is what we call, inelastic, which should not be confused with the emission of fluorescence, because it always emits at the same wavelength, regardless of the excitation [23]. Despite this marked difference, the lower intensity of the inelastic signal is one of the main obstacles when detecting a Raman signal. Once the emission occurs, it is necessary to eliminate or attenuate Rayleigh scattering, since only 1 in 1000 photons is inelastic. The inelastic signal could be perceived as noise compared to the amplitude of the elastic signal [24].

In order to attenuate the Rayleigh scattering, a pair of filters were used, the first is the same one that deflects the beam $90°$, however this filter does not block efficiently all Rayleigh radiation, whereby a second filter (Rapid Edge Omega.Inc, cut-on=540nm) was positioned parallel to the microscope field of view to clean the remaining radiation. The Schmidt prism compensates the inclination angle of the stereoscope objective lenses to couple with the eyepieces.

For the CCD sensor of the camera, it was necessary to use a negative lens in order to capture the image of the sample produced by the equipment and cover most of the sensor area. As was mentioned before, the main objective is to capture certain spectral Raman bands, corresponding to characteristic vibrational modes of the β-1,3-glucan and chitin. To do this the bandpass filters were attached directly to the lens of the CCD sensor. Both filters allow to eliminate the residual Rayleigh radiation and at the same

121 time isolates the spectral region of interest. The spectrometer was attached to the other eyepiece with only
122 the dichroic mirror and the Edge filter intercepting its optical path.

123

124 *3.2. Mycosphaerella fijiensis detection*

125 The first stage of the experiment consisted of analyzing the interaction of the laser light with the
126 microorganism. This is done to establish the possibility of getting inelastic scattering information suitable
127 for the phytopathogen detection. The samples were provided by Vegetal Biotechnology of the Universidad
128 Nacional de Colombia and tagged as Control, C139 and 080930, the last two corresponds to the artificially
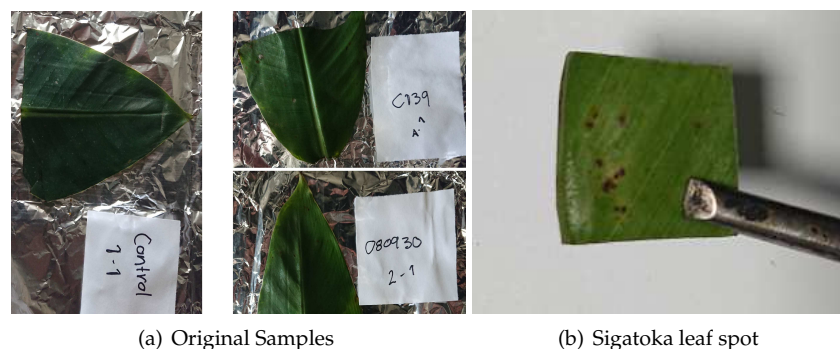129 infected specimens, as shown in Figure 3.

130

(a) Original Samples   (b) Sigatoka leaf spot

Figure 3. Infected leafs with *M. fijiensis* (080930, C139) and Control

131 For each sample, a picture was taken with and without a bandpass filter in order to capture
132 the inelastic scattering in the region of 893 cm^{-1} and the whole inelastic spectral response of the
133 sample respectively. These were obtained in order to understand the differences between the
134 two pictures and determine the types of images used in the deep learning training. The selection of
135 images is based on the amount of spectral features needed to determine the presence of the phytopathogen.

136

137 Figure 4 shows the pictures taken (without filters) of an infected sample and control

138 The black spot in figure 4 b) corresponds to one of the injuries observed in figure 3 b). The laser
139 highlights two of those spots, providing some evidence about the possibilities of laser light in the
140 phytosanitary diagnosis. However, the intention is to demonstrate if the inelastic scattering could give
141 information about the presence of these organisms. A spectrum of the injures was taken showing the
142 following features, see figure 5

143 As mentioned earlier, the main Raman bands for chitin and $\beta - 1, 3-$glucan are the ones associated
144 with the respective ν-C=O stretching of the peptide bonds (Amid I) and β C-H bending vibrations [21].
145 [22]. These signals are typically found at 1655 cm^{-1} and 893 cm^{-1} respectively. In Figure 5, two peaks
146 with those features are observed at (1563.81-897.91) cm^{-1}. It is, therefore, plausible to affirm that these
147 corresponds to the CO and CH stretch vibrational modes of the chitin and β-1,3-glucan molecules. Thus,
148 we demonstrate that by selecting the correct filters, we can observe corresponding features in the spectral
149 images as well..
150 Further images analysis will provide definitive evidence about the advantages of using this device for
151 the detection of phytopathogens. After the image processing to increase the intensity level through an
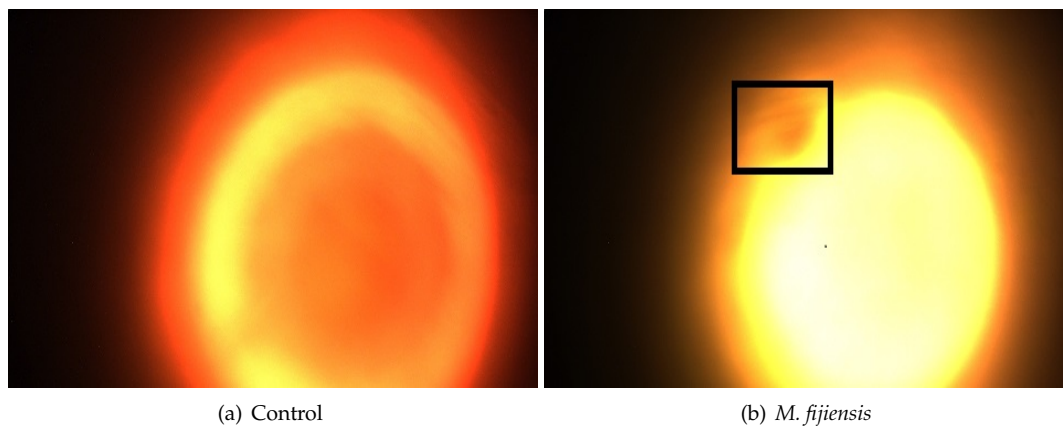
(a) Control

(b) *M. fijiensis*
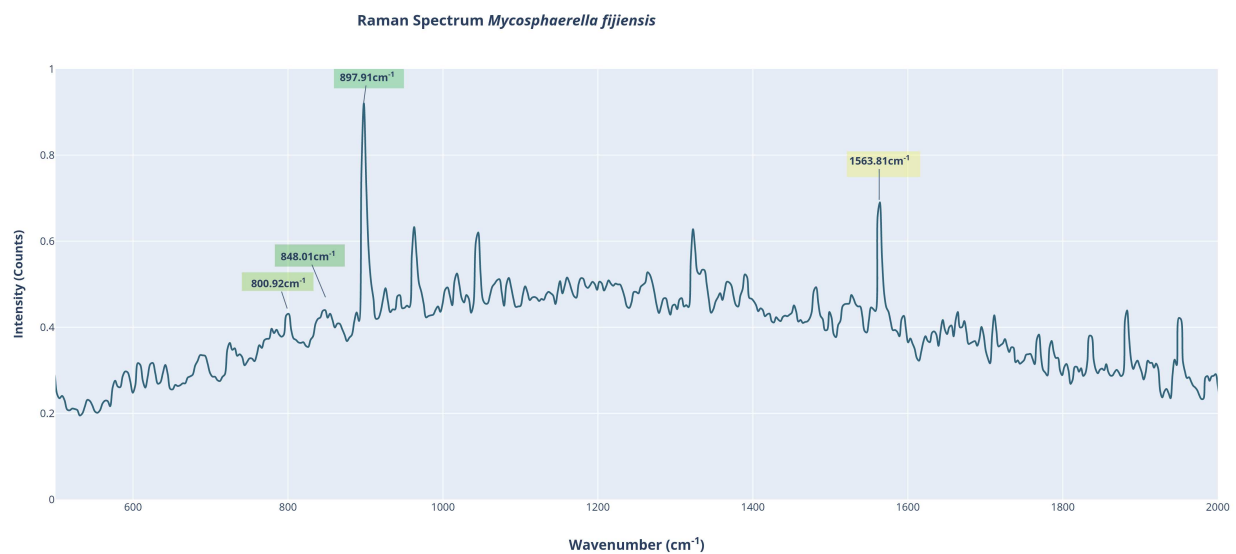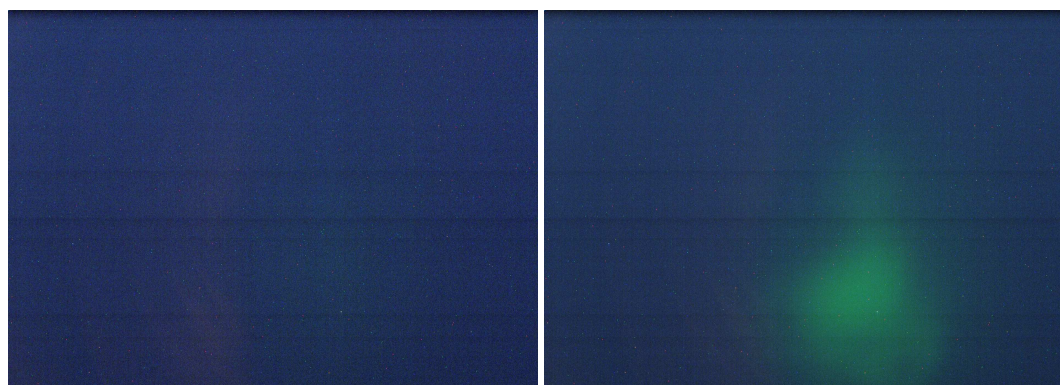
Figure 4. Pictures Without filters

Figure 5. Inelastic Spectrum of *P. fijiensis*
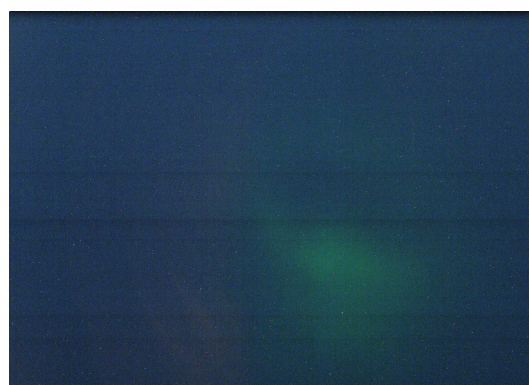
152 averaged sum of frames to simulate a increase in the exposure time, the results were the following 6:

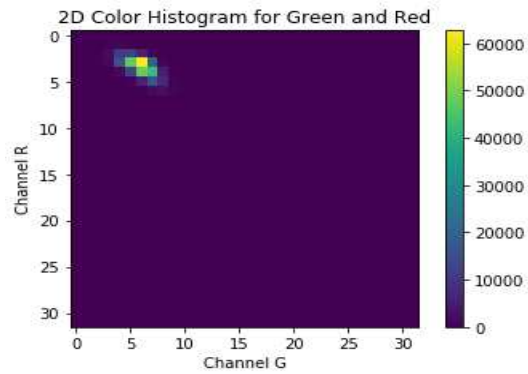**153**

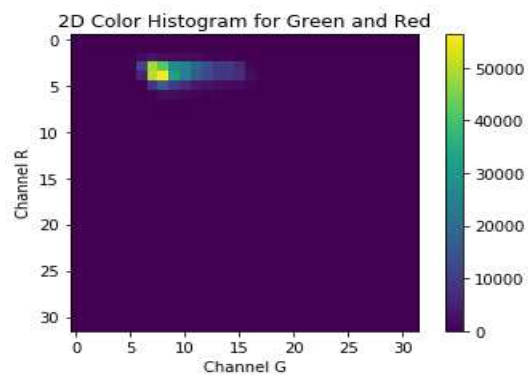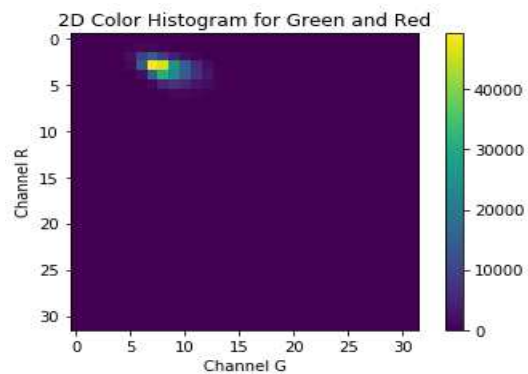(a) Control   (b) *P. fijiensis* 557 nm filter 080930 sample

(c) *P. fijiensis* 557 nm filter c139 sample

Figure 6. *P.fijiensis* control and two samples with 557nm filter and gamma correction

154 The difference with respect to the control under the same conditions of illumination (532 nm,
155 FWHM=3 nm, 112.5 mW) brings conclusive results about the presence of the microorganism in the
156 different samples. Nevertheless, an analysis of the ratio can be made between red and green channels. By
157 creating a protocol to handle all the process of phytopathogens diagnosis, a 2D histogram (just like in
158 figure 7) shows the response of the sensor in those channels specifically.

(a) Control 2D

(b) *P.fijiensis* 557 nm filter 080930 sample 2D

(c) *P.fijiensis* 557 nm filter c139 sample

Figure 7. *P.fijiensis* control and two samples with 557nm filter 2D

159   The methodology of image processing shows significant differences between samples and control.
160 Though there is a signal coming from the control, the distribution with respect to the red channel is

different as in the case of the infected samples. Their 2D histograms show similar behavior in both cases, which is a tendency towards the green channel. This is more evident for the sample 080930, but it is also perceptible for C139. The next step was to develop an automated protocol to distinguish between diseased from healthy tissue. The classification process was made with a CNN (convolutional neural network) trained with 100 images of each label with different intensity levels and changing the position in order to produce an effective learning pattern based on the spectral features only instead of geometrical or illumination conditions. For this experiment, two sample holders were prepared, one with PDA agar, the other one with small colonies of *P.fijiensis* (10 days of incubation) growing in the same type of culture media.

The network was trained to classify four different tags, agar578, agar 557, to learn the spectral features of the PDA culture media and Mycos557, Mycos578 to produce a classification model of the phytopathogen, the numbers 557, 578 corresponds to the filters which were used to take the pictures. Each image was taken with the following parameters: exposure time 1.6s, gain 54dB, once completed this process, the four sets of images were uploaded and the training process begins. The selected training parameters were 10000 training steps, a ReLu activation function and a learning rate of 0.01 which was selected after checking the behavior of the loss function (cross entropy) with different values. The batch size selected uses the entire validation set for each accuracy computation. Also, every image was randomly cropped and scaled helping the network to cope with many possible distortions of the sample images, finally the machine learning library used was PNASNet a module with a self-contained piece of a TensorFlow graph based on a sequential optimization, that can be reused in a process called transfer learning. The table 1 shows the evolution of network learning in different iterations after two hours. In figure 8 a sample of the training set for each label is shown.

8 shows the images taken with different filters after two hours of training.

Training Parameters				
Parameter	Iteration			
	1	3780	3790	9999
Train Accuracy %	76.5	100	100	100
Cross Entropy	1.29	0.00245	0.00244	0.00095
Validation Accuracy %	89.6	100	100	100

Table 1. Training Parameters for Different Iterations

The final iteration shows a successful reduction of the cross-entropy a parameter that describes how accurate is the model in the estimation of the images features. If the machine is classifying correctly, then the value of the cross-entropy will be reduced as is shown in the different iterations. Another way to interpret this is that the system is converging to the selected label. To test the training randomly selected samples of each of the tags were selected, none of them were used previously for the training, in the tables 2, 3, 4, 5 the results for each sample are shown.

P.fijiensis, 557 nm filter			
% of Recognition			
Tag	Assay 1	Assay 2	Assay 3
Agar 557	0.041	0.012	0.069
Agar 578	0.092	0.008	0.064
Mycos 557	99.81	99.97	99.83
Mycos 578	0.026	0.007	0.037
Image identified	yes	yes	yes

Table 2. Classification for *P.fijiensis* Image Taken with a 557 nm filter
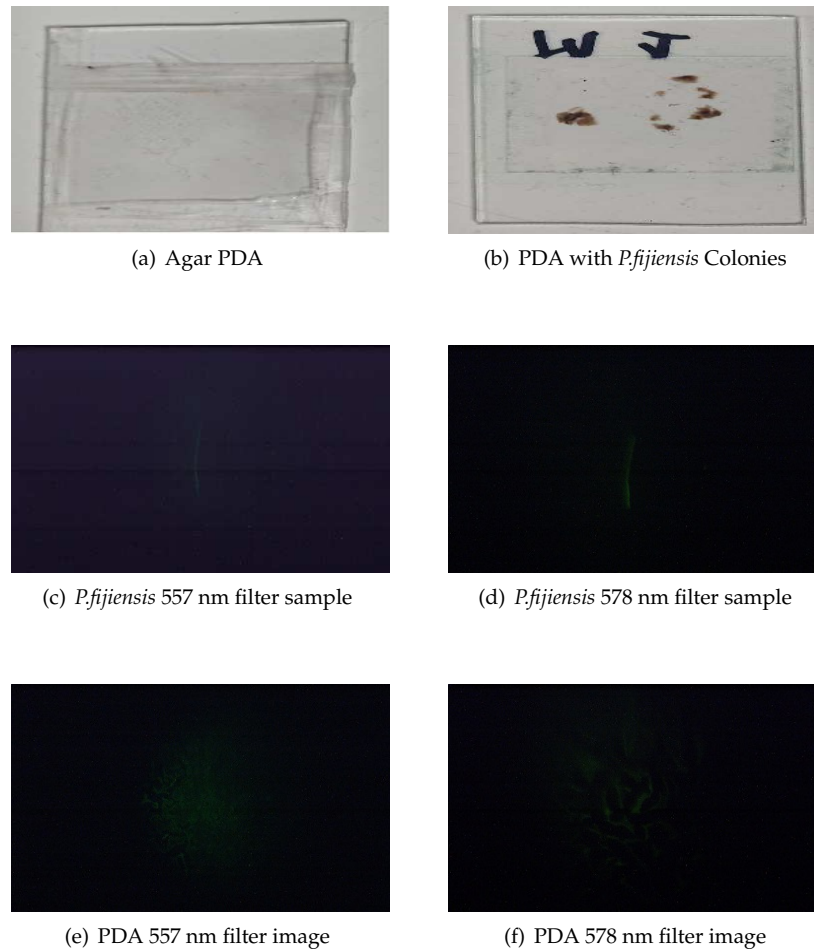
(a) Agar PDA

(b) PDA with *P.fijiensis* Colonies

(c) *P.fijiensis* 557 nm filter sample

(d) *P.fijiensis* 578 nm filter sample

(e) PDA 557 nm filter image

(f) PDA 578 nm filter image

Figure 8. *P.fijiensis* training set with different filters

P.fijiensis, 578 nm filter			
% of Recognition			
Tag	Assay 1	Assay 2	Assay 3
Agar 557	0.004	0.002	0.007
Agar 578	0.017	0.003	0.057
Mycos 557	0.002	0.001	0.004
Mycos 578	99.97	99.99	99.93
Image identified	yes	yes	yes

Table 3. Classification for *P.fijiensis* Image Taken with a 578nm filter

Agar 557 nm			
% of Recognition			
Tag	Assay 1	Assay 2	Assay 3
Agar 557	99.89	99.98	98.89
Agar 578	0.065	0.016	0.283
Mycos 557	0.004	0.001	0.006
Mycos 578	0.033	0.005	0.823
Image identified	yes	yes	yes

Table 4. Classification for Agar Image Taken with a 557nm filter

Agar 557nm			
% of Recognition			
Tag	Assay 1	Assay 2	Assay 3
Agar 557	0.009	0.006	0.023
Agar 578	99.98	99.83	99.82
Mycos 557	0.002	0.001	0.009
Mycos 578	0.008	0.17	0.148
Image identified	yes	yes	yes

Table 5. Classification for Agar Image Taken with a 578nm filter

190   In all cases, the neural network was able to successfully identify the presence of *Pseudocercospora*
191 *fijiensis* with a certainty higher than 98%, which was the general purpose of this work. Each of the tables
192 has in the upper part a label that indicates, the experiment carried out, for example, the table 2 shows in
193 the first row the classification carried out by the algorithm for three different images, in the first test, the
194 system was able to recognize the spectral pattern left by the microorganism with 99.81% of certainty, for
195 that particular image, this image was not supplied to the machine for training, it was taken later and
196 effectively corresponds to the label indicated, this leads to the conclusion that the system has the potential
197 to correctly classify a sample. Similar results were obtained for each experiment performed with other
198 testing images showing that the system can differentiate healthy tissue from diseased. It should be noted
199 that this percentage occurred under controlled conditions of experimentation as those mentioned in the
200 methodology.

201

202 In summary, after the training with the spectral images, all the times that the system was supplied with
203 images with different infected structures or not, it was able to respond correctly, regardless of the type of
204 filter or sample, the reason for this is that each image creates a very particular distribution of intensities in
205 the corresponding color channels, making it possible to "learn" to differentiate these characteristics, so
206 with a deeper training and in different conditions, it would be possible to generate a system capable of

207 executing this task in the countryside or industry.

208

209

4. Conclusions

211   A set of tools was developed to create a system capable of detecting phytopathogens of fungal
212 origin, combining algorithms for image processing, electronics, optics, deep learning techniques, and
213 mechanical design. The whole system is a synergy of those elements that together with the knowledge of
214 the phenomenology of inelastic scattering, introduces into the Colombian agriculture a design that could
215 compete with similar solutions of foreign origin.

216 The strategy in the selection of filters, allowed us to limit the set of wavenumbers to regions where the
217 possible inelastic signals associated with fungal phytopathogens are manifested exclusively, allowing it to
218 establish their presence both individually and on plant tissue, the aforementioned strategy was based on
219 the review of dozens of similar works related with the fungal wall biochemistry, which was the cellular
220 structure most exposed to laser radiation.

221 Additionally, the image processing algorithms proved to be an excellent complement in the analysis of the
222 Raman scattering signal, which shows that the use of a spectrometer is not necessary once the system is
223 already calibrated. In the experiments with *P.fijiensis*, the operations on the image and the subsequent
224 deep learning training gave the computer the capacity to evaluate the image features and determine if the
225 phytopathogen is on the plant tissue.

226

227

References

237 1.   MANZO-SÁNCHEZ, G., et al. Biology of Mycosphaerella fijiensis Morelet and its interacción with Musa spp.
238   Revista Mexicana de Fitopatología, **2005**, vol. 23, no 1, p. 87-96.

239 2.   HERRERA, M. Manejo y control de la Sigatoka negra en plátano y banano. Revista ASIAVA, **2007**, vol. 77, p.
240   12-15.

241 3.   MOURICHON, X., et al. Geographical distribution of the two species Mycosphaerella musicola Leach
242   (Cercospora musae) and M. fijiensis Morelet (C. fijiensis), respectively agents of Sigatoka disease and black leaf
243   streak disease in bananas and plantains. Fruits, **1990**, vol. 45, no 3, p. 213-218.

244 4.   RHODES, P. L., et al. A new Banana disease in Fiji. Commonwealth Phytopathological News, *1964*, vol. 10, no 3,
245   p. 38-41.

246 5.   STOVER, R. H., et al. Distribution and probable origin of Mycosphaerella fijiensis in southeast Asia. Tropical
247   Agriculture, Trinidad and Tobago, *1978*, vol. 55, no 1, p. 65-68.

248 6.   MAHECHA-VÁSQUEZ, Germán; SIERRA, Sair; POSADA, Raúl. Diversity indices using arbuscular mycorrhizal
249   fungi to evaluate the soil state in banana crops in Colombia. Applied soil ecology, *2017*, vol. 109, p. 32-39.

250 7.   Agronet, M. Estadísticas Agropecuarias. Retrieved from http://www.agronet.gov.co/estadistica/Paginas/home.
251   aspx.*2019*

252 8.   AMAYA, Catalina María Zuluaga; HOYOS, Luis Fernando Patiño; VILLA, Juan Carlos Collazos. Integración de
253   inducción de resistencia con bacterias quitinolíticas en el control de la sigatoka negra (mycosphaerella fijiensis
254   morelet) en banano. Revista Facultad Nacional de Agronomía Medellín, *2007*, vol. 60, no 2, p. 3891-3905.

255 9.   FREE, Stephen J. Fungal cell wall organization and biosynthesis. En Advances in genetics. Academic Press, *2013*.
256   p. 33-82.

257 10. NOOTHALAPATI, Hemanth, et al. Label-free chemical imaging of fungal spore walls by Raman microscopy and
258   multivariate curve resolution analysis. Scientific reports, *2016*, vol. 6, p. 27789.

259 11. LOUDON, Rodney. The quantum theory of light. OUP Oxford, *2000*.

260 12. BERNATH, Peter F. Spectra of atoms and molecules. Oxford university press, *2015*.

261 13. LONG, Derek A. The Raman effect—a unified treatment of the theory of Raman scattering by molecules. Derek
262   A. Long, John Wiley & Sons, Ltd., *2002*, Pp 597. ISBN 0-471-49028-8.

263 14. SOCRATES, George. Infrared and Raman characteristic group frequencies: tables and charts. John Wiley & Sons,
264   *2004*.

265 15. CZAMARA, Krzysztof, et al. Raman spectroscopy of lipids: a review. Journal of Raman Spectroscopy, *2015*, vol.
266   46, no 1, p. 4-20.

267 16. WIERCIGROCH, Ewelina, et al. Raman and infrared spectroscopy of carbohydrates: A review. Spectrochimica
268   Acta Part A: Molecular and Biomolecular Spectroscopy, *2017*, vol. 185, p. 317-335.

269 17. KE, Yan, et al. PCA-SIFT: A more distinctive representation for local image descriptors. CVPR (2),*2004*, vol. 4, p.
270   506-513.

271 18. ZHANG, Daoqiang; ZHOU, Zhi-Hua. (2D) 2PCA: Two-directional two-dimensional PCA for efficient face
272   representation and recognition. Neurocomputing, *2005*, vol. 69, no 1-3, p. 224-231.

273 19. LIU, Chenxi, et al. Progressive neural architecture search. En Proceedings of the European Conference on
274   Computer Vision (ECCV). *2018*. p. 19-34.

275 20. ZOPH, Barret, et al. Learning transferable architectures for scalable image recognition. En Proceedings of the
276   IEEE conference on computer vision and pattern recognition. *2018*. p. 8697-8710.

277 21. NOOTHALAPATI, Hemanth, et al. Label-free chemical imaging of fungal spore walls by Raman microscopy and
278   multivariate curve resolution analysis. Scientific reports, 2016, vol. 6, p. 27789.

279 22. WYSOKOWSKI, Marcin, et al. Isolation and identification of chitin in three-dimensional skeleton of Aplysina
280   fistularis marine sponge. International journal of biological macromolecules, 2013, vol. 62, p. 94-100.

281 23. CLARKE, Ronald J.; OPRYSA, Anna. Fluorescence and light scattering. Journal of chemical education, 2004, vol.
282   81, no 5, p. 705.

283 24. HARRIS, Daniel C.; BERTOLUCCI, Michael D. Symmetry and spectroscopy: an introduction to vibrational and
284   electronic spectroscopy. Courier Corporation, 1989.

285 25. BERNREITER, Andreas. Molecular diagnostics to identify fungal plant pathogens–a review of current methods.
286   ECUADOR ES CALIDAD-Revista Científica Ecuatoriana, 2017, vol. 4.

287 26. SNEHALATHARANI, A.; KHAN, A. N. A. Biochemical and physiological characterisation of Erwinia species
288   causing tip-over disease of banana. Archives Of Phytopathology And Plant Protection, 2010, vol. 43, no 11, p.
289   1072-1080.

290 32. JOHANSON, A.; JEGER, M. J. Use of PCR for detection of Mycosphaerella fijiensis and M. musicola, the causal
291   agents of Sigatoka leaf spots in banana and plantain. Mycological research, 1993, vol. 97, no 6, p. 670-674.

292 33. SEAL, S. E., et al. Determination of Ralstonia (Pseudomonas) solanacearum rDNA subgroups by PCR tests. Plant
293   Pathology, 1999, vol. 48, no 1, p. 115-120.

294 35. PIEPENBURG, Olaf, et al. DNA detection using recombination proteins. PLoS biology, 2006, vol. 4, no 7, p. e204.

295 30. BERNREITER, Andreas. Molecular diagnostics to identify fungal plant pathogens–a review of current methods.
296   ECUADOR ES CALIDAD-Revista Científica Ecuatoriana, 2017, vol. 4.

31. SNEHALATHARANI, A.; KHAN, A. N. A. Biochemical and physiological characterisation of Erwinia species causing tip-over disease of banana. Archives Of Phytopathology And Plant Protection, 2010, vol. 43, no 11, p. 1072-1080.

32. JOHANSON, A.; JEGER, M. J. Use of PCR for detection of Mycosphaerella fijiensis and M. musicola, the causal agents of Sigatoka leaf spots in banana and plantain. Mycological research, 1993, vol. 97, no 6, p. 670-674.

33. SEAL, S. E., et al. Determination of Ralstonia (Pseudomonas) solanacearum rDNA subgroups by PCR tests. Plant Pathology, 1999, vol. 48, no 1, p. 115-120.

34. EL WAHED, Ahmed Abd, et al. A portable reverse transcription recombinase polymerase amplification assay for rapid detection of foot-and-mouth disease virus. PloS one, 2013, vol. 8, no 8, p. e71642.

35. PIEPENBURG, Olaf, et al. DNA detection using recombination proteins. PLoS biology, 2006, vol. 4, no 7, e204.

36. ALVAREZ, Javier C., et al. Characterization of a differentially expressed phenylalanine ammonia-lyase gene from banana induced during Mycosphaerella fijiensis infection. Journal of Plant Studies, 2013, vol. 2, no 2, p. 35

37. BINYAMINI, N.; SCHIFFMANN-NADEL, Mina. Latent infection in avocado fruit due to Colletotrichum gloeosporioides. Phytopathology, 1972, vol. 62, no 6, p. 592-594.

Sample Availability: Samples of the compounds ...... are available from the authors.